J. Fluid Mech. (1976), *vol.* 78, *part* 4, *pp.* 763–784
Printed in Great Britain

The occurrence of parametric instabilities in finite-amplitude internal gravity waves

By RICHARD P. MIED

Ocean Sciences Division, Naval Research Laboratory, Washington, D.C. 20375

(Received 3 October 1975)

The parametric instability of a plane internal gravity wave is considered. When the two-dimensional equations of vorticity and mass conservation are linearized in the disturbance quantities, partial differential equations with periodic coefficients result. Substitution of a perturbation of the form dictated by Floquet theory into these equations yields compatibility conditions which, when evaluated numerically, give the curves of neutral stability and constant disturbance growth rate. These results reveal that, for an internal wave of even infinitesimal amplitude, disturbance waves can begin to grow in amplitude. Moreover, these parametric instabilities are shown to reduce to the classical case of the nonlinear resonant interaction in the limit of vanishingly small basic-state amplitude. The fact that these unstable disturbances can exist for an internal wave of any amplitude suggests that this phenomenon may be an important mechanism for extracting energy from an internal gravity wave.

1. Introduction

In the deep ocean, internal gravity waves provide a mechanism which is responsible for the transport of momentum and energy over appreciable distances without any significant net movement of mass. As the ubiquity of these waves is a matter of record (Garrett & Munk 1972), one is inclined to investigate the nature of any phenomena that would impair, or at least impede, their ability to propagate. In the case of waves with a group velocity directed upwards, for example, Booker & Bretherton (1967) have shown that above the height at which the mean horizontal velocity equals the horizontal phase speed of the wave, the so-called critical level, very little energy is transmitted. This critical layer is regarded as a sink of wave energy, although Thorpe (1975) mentions that no experimental evidence exists to show that the deficit in wave momentum will appear in the basic flow. In a somewhat different vein, Breeding (1971) has shown that a significant amount of the wave energy impinging on the critical layer can be reflected there, although several other naturally occurring phenomena can produce a similar effect. For example, even under propagation conditions which preclude the existence of a critical layer, horizontal shears and the thermocline itself can reflect significant fractions of the internal-wave energy incident upon them from above or below (Mied & Dugan 1974, 1975).

In addition to the reflexion of energy, various instabilities arising from the

wave motion itself can interfere with the wave propagation. The debate over which of the several types of instability are predominantly responsible for any disintegration of waves in the ocean is a lively one. The mechanism first proposed was that of the shear-flow instability. Assuming that the amplitude of each individual wave trapped on the thermocline is limited by the occurrence of a Kelvin–Helmholtz instability at its crests and troughs, Phillips (1966*a*) has calculated a spectral shape which is in fair agreement with the results of Charnock (1965) for towed spectra. Orlanski & Bryan (1969) later pointed out that, if the wave-related horizontal speed of a fluid particle anywhere equals the horizontal propagation velocity, a local overturning of the density structure might occur. Applying this amplitude-limiting criterion to each Fourier component individually, Orlanski (1971) derived a spectrum which, like Phillips's, is in fair agreement with Charnock's towed wave spectra. On the other hand, McEwan & Robinson (1975) criticize Orlanski (1972) for having neglected fine-scale structure in his analytical model of overturning in standing internal waves. They point out in this regard that a common form of internal-wave instability is a rather delicate one which manifests itself in those nonlinearities neglected by Orlanski. To focus upon this phenomenon better, McEwan & Robinson model the basic-state wave by a periodic rotation of the isopycnals and thus restrict their attention to potentially unstable disturbances having length scales much smaller than those of the basic wave motion whose stability they are investigating. By so doing they demonstrate that these small-scale wavelets are parametrically unstable to the local rocking motion of the isopycnals, which models the local effect of the large-scale wave. Viscosity is essential in determining disturbance growth rates in this calculation and so the instability is considered important in the formation of oceanic fine-structure having scales of the order of centimetres.

In the present paper, we investigate the stability of finite-amplitude plane monochromatic internal gravity waves and, further, the mechanism upon which we focus our attention is that of a parametric instability. Although the present analysis neglects nonlinear disturbance terms, we shall make no restrictions on the length scales of these unstable wavelets. Without these *a priori* disturbance length-scale arguments, the analytical solution of the problem is quite complex, as was noted by McEwan & Robinson. The approach we shall take, therefore, is a numerical one and this allows the examination of the stability of finite-amplitude internal waves with any length scale and presumably allows us to obtain results to arbitrary accuracy.

2. A simple example

The coupled partial differential equations describing internal-wave instabilities are formidable, and the search for their modes of parametric instability does not appear straightforward. A careful examination of the well-known Mathieu equation provides an excellent opportunity to observe the properties of these parametric instabilities in a simple one-dimensional equation; moreover, this simple case will suggest the appropriate methods to be employed in the internal-wave problem.

Mathieu function	$N = 3$	$N = 5$	$N = 7$
$\mathrm{ce}_0(\eta, M)$	$\alpha = O(M)$	$\alpha = -\frac{1}{2}M^2 + O(M^4)$	$\alpha = -\frac{1}{2}M^2 + O(M^4)$
$\mathrm{ce}_1(\eta, M)$	$\alpha = 1 + M + O(M^2)$	$\alpha = 1 + M + O(M^2)$	$\alpha = 1 + M - \frac{1}{8}M^2 + O(M^3)$
$\mathrm{se}_1(\eta, M)$	$\alpha = 1 - M + O(M^2)$	$\alpha = 1 - M + O(M^2)$	$\alpha = 1 - M - \frac{1}{8}M^2 + O(M^3)$
$\mathrm{ce}_2(\eta, M)$		$\alpha = 4 + \frac{1}{2}M^2 + O(M^4)$	$\alpha = 4 + \frac{1}{2}M^2 + O(M^3)$
$\mathrm{se}_2(\eta, M)$		$\alpha = 4 + O(M^2)$	$\alpha = 4 + O(M^2)$
$\mathrm{ce}_3(\eta, M)$			$\alpha = 9 + \frac{1}{8}M^2 + O(M^3)$
$\mathrm{se}_3(\eta, M)$			$\alpha = 9 + \frac{1}{8}M^2 + O(M^2)$

TABLE 1. The neutral curves $\alpha = \alpha(M)$ of Mathieu's equation shown for varying determinant order N and Mathieu functions ce_n and se_n (notation of Abramowitz & Stegun 1965). The neutral curve for ce_2 is still in error (for $N = 7$) by $\frac{1}{128}M^2$, the correct result being $\alpha = 4 + \frac{5}{128}M^2 + O(M^4)$.

Mathieu's equation (Ince 1956) is written as

$$\psi_{\eta\eta} + (\alpha - 2M\cos 2\eta)\psi = 0. \tag{1}$$

If $M = 0$, (1) admits a solution of period π or 2π when $\alpha = n^2$, where n is any integer. All periodic solutions to (1) are not necessarily stable, however, and we anticipate this behaviour by assuming a solution of the form

$$\psi = \exp(\mu\eta) \sum_{n=-\infty}^{\infty} \psi_n e^{in\eta}.$$

Substitution of this expression into (1) will yield a set of compatibility conditions $\alpha = \alpha(M; \mu)$ which indicate how the parameters of the assumed solution are related. These expressions $\alpha = \alpha(M; \mu)$ represent curves of $\mu =$ constant in the α, M plane (Abramowitz & Stegun 1965). In particular, the curves on which $\mu = 0$ separate the regions of stable (purely imaginary μ) and unstable solutions (complex μ) to (1) in this α, M plane. We may calculate these neutral curves $\alpha = \alpha(M)$ by setting $\mu = 0$ and writing

$$\psi = \sum_{n=-\infty}^{\infty} \psi_n e^{in\eta}. \tag{2}$$

Substituting (2) into (1) and re-indexing the sums, we obtain the recursion relation

$$-M\psi_{n-2} + (\alpha - n^2)\psi_n - M\psi_{n+2} = 0, \quad n = 0, \pm 1, \pm 2, \ldots .$$

For each integer, we obtain an equation linking the three non-contiguous mode coefficients ψ_{n-2}, ψ_n and ψ_{n+2}. These equations are homogeneous, however, and the necessary condition for a non-trivial solution to exist is that an infinite determinant Δ vanish (see appendix):

$$\Delta(\alpha, M; N = \infty) = 0, \tag{3}$$

where N is the order of the determinant. This condition then establishes the manner in which α and M must be related so that the periodic solution (2) can satisfy (1). By taking ever larger determinants from the centre of (3), we can obtain a progressively more accurate approximation to these curves of neutral

stability, these curves emerging from the calculation as asymptotic series in M. Somewhat surprisingly, a significant amount of information is obtained by evaluating (3) when $N = 3$, and table 1 shows the neutral curves obtained for $N = 3$, 5 and 7. Calculation of $\Delta(\alpha, M; N = 7) = 0$ is as far as we may proceed without incurring considerable difficulty, but the trend is clear. As we increase N, more parametric relations are discovered, and generally the accuracy to which we know those curves previously found is improved. Unfortunately, it is also obvious that the analytical solution of a more complicated equation would be very difficult to obtain in this fashion, particularly if we also seek the $\mu =$ constant curves in the α, M plane.

In the section below, we shall approach the problem of internal-wave stability by assuming a form of the solution which is suggested by the wavelike character of the basic state; however, a much more imposing determinant will arise. For this problem we seek not only the curves of neutral stability, but those of constant disturbance growth rate as well. The complexity of the problem and the accuracy desired in this work require that we calculate the determinant numerically using complex arithmetic.

3. Parametric instabilities in internal waves

3.1. *Theory*

In the Boussinesq approximation, the two-dimensional inviscid equations governing the motion of an incompressible density-stratified fluid can be written (Phillips 1968) as

$$\nabla^2\Psi_t + B_x = \partial(\Psi, \nabla^2\Psi)/\partial(x, y), \tag{4a}$$

$$B_t - N^2\Psi_x = \partial(\Psi, B)/\partial(x, y), \tag{4b}$$

where x and y are the horizontal and vertical co-ordinates, $\nabla^2 = \partial^2/\partial x^2 + \partial^2/\partial y^2$, N is the Brunt–Väisälä frequency,† the stream function Ψ is defined such that the velocity $\mathbf{u} = (\Psi_y, -\Psi_x)$, and the buoyancy B is specified in terms of the gravity g, the reference-state density ρ_0 and the local fluid density ρ as

$$B = -g(\rho - \rho_0)/\rho_0.$$

In a constant-N fluid, (4) admits the well-known plane-wave solution

$$\Psi = A\cos(lx + my - \omega t), \tag{5a}$$

$$B = -N^2 lA\,\omega^{-1}\cos(lx + my - \omega t), \tag{5b}$$

where $\mathbf{k} = (l, m)$ is the wavenumber. The dispersion relation is given by

$$\omega/N = l/|\mathbf{k}| = \cos\theta, \tag{6}$$

θ being the angle that $\mathbf{k}$ makes with the horizontal. By virtue of the incompressibility of the fluid, $\mathbf{u}$ is perpendicular to $\mathbf{k}$ and so the nonlinear terms vanish identically. The wave whose form is given by (5) is thus a solution to the full

† N is also used to indicate the order of the determinant; the two uses are so disparate that no confusion should arise from this.

nonlinear equations (4). This fact affords us the opportunity to examine the stability of a finite-amplitude plane internal gravity wave. To do so, we express the stream function and buoyancy field as the sum of the basic state and a perturbation. Thus

$$\Psi = A\cos(lx+my-\omega t)+\psi, \tag{7a}$$

$$B = -N^2lA\omega^{-1}\cos(lx+my-\omega t)+b. \tag{7b}$$

Substituting (7) into (4) and neglecting terms which are nonlinear in the disturbance quantities ψ and b, we obtain

$$\nabla^2\psi_t+b_x = -A\sin\phi\{l\nabla^2\psi_y-m\nabla^2\psi_x+k^2[l\psi_y-m\psi_x]\},$$

$$b_t-N^2\psi_x = -A\sin\phi\{lb_y-mb_x+N^2l^2\omega^{-1}\psi_y-N^2lm\omega^{-1}\psi_x\},$$

where $\phi = lx+my-\omega t$ and $k = |\mathbf{k}|$. It is convenient to introduce the non-dimensional variables $\tilde{\psi}$, $\tilde{b}$, $\tilde{x}$, $\tilde{y}$ and $\tilde{t}$ as follows:

$$\psi = Nk^{-2}\tilde{\psi}, \quad (x,y) = k^{-1}(\tilde{x},\tilde{y}), \quad b = N^2k^{-1}\tilde{b}, \quad t = N^{-1}\tilde{t}.$$

If we define $M = Ak^2/2N$ as a measure of the basic-state amplitude and delete the tilde above the dependent and independent variables, the non-dimensional equations are

$$\nabla^2\psi_t+b_x = -2M\sin\phi\,[\cos\theta\,\nabla^2\psi_y-\sin\theta\,\nabla^2\psi_x+\cos\theta\,\psi_y-\sin\theta\,\psi_x], \tag{8a}$$

$$b_t-\psi_x = -2M\sin\phi\,[\cos\theta\,\psi_y-\sin\theta\,\psi_x+\cos\theta\,b_y-\sin\theta\,b_x]. \tag{8b}$$

These are the disturbance equations and we note that, in the absence of a basic flow ($M = 0$), the disturbance quantities ψ and b take the forms which describe freely propagating internal waves.

We may simplify (8) by expressing them in a co-ordinate system which is more suggestive of the fundamental internal-wave geometry. Let us therefore introduce a rotated system (ξ,η), which is oriented such that the $+\eta$ axis coincides with the direction of phase propagation (see figure 1*a*). Then

$$\xi = x\sin\theta-y\cos\theta, \quad \eta = x\cos\theta+y\sin\theta,$$

and under this transformation, (8) become

$$\nabla^2\psi_t+(\sin\theta\,b_\xi+\cos\theta\,b_\eta) = 2M\sin\phi\,(\psi_\xi+\nabla^2\psi_\xi), \tag{9a}$$

$$b_t-(\sin\theta\,\psi_\xi+\cos\theta\,\psi_\eta) = 2M\sin\phi\,(\psi_\xi+b_\xi), \tag{9b}$$

where $\nabla^2 = \partial^2/\partial\xi^2+\partial^2/\partial\eta^2$ and $\phi = \eta-t\cos\theta$. The basic state is now specified by $\Psi = 2M\cos\phi$ and $B = -2M\cos\phi$, and the parameter M is seen to appear before those terms in (9) which couple the basic state with the perturbation (ψ,b); the apparent similarity between (1) and (9) is thus reinforced. This system of partial differential equations describes the behaviour of a disturbance (ψ,b) to a plane internal gravity wave. The form of this perturbation suggests itself if we examine the nature of the basic-state wave motion, which is that of a wave-associated velocity field propagating without change of form.

We note that the system (9*a* and *b*) will admit a separated solution of the form

$$(\psi,b) = f_1(t)f_2(\xi)f_3(\phi).$$

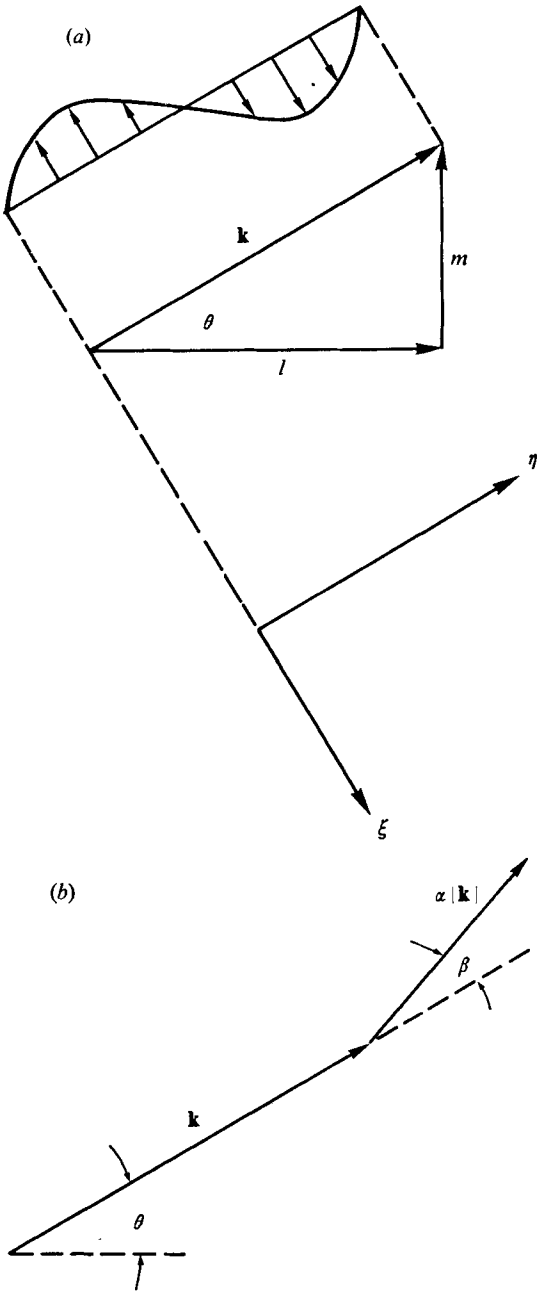

FIGURE 1. (*a*) The wave-related velocity profile $-2M \sin(\eta - t\cos\theta)$ propagates without change of form through the fluid. The $+\eta$ axis in the rotated ξ, η co-ordinate system is aligned in the direction of the phase propagation of the wave. (*b*) The Floquet vector having magnitude α propagates at an angle β to the basic state with normalized wavenumber (0, 1).

Because of the appearance of periodic coefficients in (9*a*, *b*), Floquet theory (Davis 1962) requires that we put

$$f_3 = \exp(\mu\phi) \sum_{n=-\infty}^{\infty} F_n e^{in\phi},$$

where μ is in general complex; this form is identical to the one appearing in §2. Let us seek solutions which are bounded in space (wavelike solutions), but which are free to grow in time. Thus we require that μ be imaginary and write the general solution as

$$\psi = \exp(\gamma t)\exp(i\phi_0) \sum_{n=-\infty}^{\infty} \psi_n \exp(in\phi),$$

$$b = \exp(\gamma t)\exp(i\phi_0) \sum_{n=-\infty}^{\infty} b_n \exp(in\phi),$$

where $\phi_0 = (-\alpha\sin\beta)\xi + (\alpha\cos\beta)\eta - \sigma_\beta t$ and the ψ_n and b_n are complex Fourier coefficients. The Floquet wave $\exp(i\phi_0)$ is thus seen to propagate with frequency σ_β at an angle β with respect to the basic-state wave (see figure 1*b*). This method of solution is analogous to the one employed by Gill (1974) in his investigation of the stability of Rossby waves on a beta-plane.

Substitution of this form into (9*a*, *b*) yields

$$\begin{aligned}
&-[\gamma - in\cos\theta - i\sigma_\beta][(\alpha\sin\beta)^2 + (\alpha\cos\beta + n)^2]\psi_n \\
&+[-i\alpha\sin\theta\sin\beta + i\cos\theta(\alpha\cos\beta + n)]b_n \\
&= \alpha M\sin\beta\{1 - [(\alpha\sin\beta)^2 + (\alpha\cos\beta + n + 1)^2]\}\psi_{n+1} \\
&-\alpha M\sin\beta\{1 - [(\alpha\sin\beta)^2 + (\alpha\cos\beta + n - 1)^2]\}\psi_{n-1}, \qquad (10a)
\end{aligned}$$

$$\begin{aligned}
&[\gamma - in\cos\theta - i\sigma_\beta]b_n - [-i\alpha\sin\beta\sin\theta + i(\alpha\cos\beta + n)\cos\theta]\psi_n \\
&\qquad = \alpha M\sin\beta\{b_{n+1} + \psi_{n+1} - b_{n-1} - \psi_{n-1}\}. \qquad (10b)
\end{aligned}$$

This system can generally be solved for a range of β somewhere within the open interval (0°, 180°); and in fact, the growth rates $\mathrm{Re}\,\gamma$ of the allowable disturbances will be functions of the angle that the Floquet vector makes with the basic-state wavenumber. The usual procedure would be to vary β to find those disturbances which grow at the maximum rate for a given basic-state amplitude $2M$ and direction θ. In this fashion, the quickest growing, and thus most dangerous, instabilities are discovered. Unfortunately, the cost of performing these calculations for even one value of β is prohibitively large. Since trial computations for a variety of values of β indicate that the qualitative features of the instability remain unaltered, there is little compromise involved in selecting one β for close examination; the significance of this restriction is discussed in §4. Thus, with little loss in generality, let us set $\beta = 90°$ for the remainder of this work so that the solution becomes

$$\psi = \exp(\lambda t)\exp(-i\alpha\xi) \sum_{n=-\infty}^{+\infty} \psi_n \exp(in\phi), \qquad (11a)$$

$$b = \exp(\lambda t)\exp(-i\alpha\xi) \sum_{n=-\infty}^{+\infty} b_n \exp(in\phi), \qquad (11b)$$

with $\lambda = \gamma - i\sigma_\beta$, and then (10*a*, *b*) become

$$\lambda_n \psi_n - p_n q_n^{-1} b_n - \alpha M[d_n \psi_{n+1} - e_n \psi_{n-1}] = 0, \tag{12a}$$

$$\lambda_n b_n - p_n \psi_n - \alpha M(b_{n+1} - b_{n-1}) - \alpha M(\psi_{n+1} - \psi_{n-1}) = 0, \tag{12b}$$

where $$p_n = i(n\cos\theta - \alpha\sin\theta), \quad q_n = n^2 + \alpha^2,$$

$$d_n = [(n+1)^2 + \alpha^2 - 1]/(n^2+\alpha^2), \quad e_n = [(n-1)^2 + \alpha^2 - 1]/(n^2+\alpha^2),$$

and $\lambda_n = \lambda - in\cos\theta$. Equation (12*a*) provides expressions for b_n, b_{n-1} and b_{n+1}, which can be substituted into (12*b*) to obtain a recursion relation linking five contiguous ψ_n:

$$\left\{\frac{\alpha^2 M^2 q_{n-1} e_{n-1}}{p_{n-1}}\right\}\psi_{n-2} + \alpha M\left\{\frac{\lambda_n q_n e_n}{p_n} + \frac{\lambda_{n-1} q_{n-1}}{p_{n-1}} + 1\right\}\psi_{n-1}$$
$$+\left\{\frac{\lambda_n^2 q_n}{p_n} - p_n - \frac{\alpha^2 M^2 q_{n+1} e_{n+1}}{p_{n+1}} - \frac{\alpha^2 M^2 q_{n-1} d_{n-1}}{p_{n-1}}\right\}\psi_n$$
$$-\alpha M\left\{\frac{\lambda_n q_n d_n}{p_n} + \frac{\lambda_{n+1} q_{n+1}}{p_{n+1}} + 1\right\}\psi_{n+1} + \left\{\frac{\alpha^2 M^2 q_{n+1} d_{n+1}}{p_{n+1}}\right\}\psi_{n+2} = 0. \tag{13}$$

By substituting the values $n = 0, \pm 1, \pm 2, \ldots, \pm N$ into (13) in turn, we obtain a system of homogeneous equations for the ψ_n, which are treated in the same fashion as those arising in § 2. For a non-trivial solution to exist, we require that the determinant of the coefficient matrix vanish, so that

$$\Delta(\alpha, \lambda, M, \theta; N) = 0. \tag{14}$$

However, there arise complications not present in (3). Not only is the determinant (14) complex but λ is also. Thus

$$\lambda = \lambda_r + i\lambda_i.$$

The imaginary part λ_i combines with the frequency of the basic-state harmonics to provide a frequency $\mathrm{Im}\,\lambda_n$ for the various parametric instabilities, so that

$$\mathrm{Im}\,\lambda_n = \lambda_i - n\cos\theta.$$

The solution of (14) will give the neutral-growth curve, as well as the curves of constant growth rate

$$\alpha = \alpha(M; \lambda_r).$$

We also suspect that λ_i is dependent on the disturbance wavenumber α, and the results of the calculations reported below bear this out. The question to which we seek an answer is then as follows. Suppose an internal wave with amplitude $2M$ has a phase which propagates at a direction $\theta\,(= \tan^{-1} m/l)$ to the horizontal. Which disturbance wavelets will grow, and what is their growth rate λ_r and frequency $\lambda_i - n\cos\theta$?

3.2. *The nature of the instability*

In our treatment of the Mathieu equation, the various branches of the neutral-stability curves, as well as the solutions valid along them, emerge as asymptotic series in M. For the case $M = 0$, the trivial result $\alpha = n^2$ is retrieved and a

neutrally stable solution emerges. When $M = 0$ in the present case, (12a, b) become

$$(\lambda - in\cos\theta)\,\psi_n - i(n\cos\theta - \alpha\sin\theta)\,(n^2+\alpha^2)^{-1}\,b_n = 0,$$

$$-i(n\cos\theta - \alpha\sin\theta)\,\psi_n + (\lambda - in\cos\theta)\,b_n = 0.$$

The condition that there be non-trivial solutions to this system is met if the respective determinants vanish, and this yields

$$\lambda_r = 0,$$

$$\lambda_i - n\cos\theta = (n\cos\theta - \alpha\sin\theta)/(n^2+\alpha^2)^{\frac{1}{2}}, \quad n = 0, \pm 1, \pm 2, \ldots . \tag{15}$$

As was anticipated in §3.1, λ_i is indeed observed to be a function of α. Further, each value of n corresponds to a different neutrally stable mode. When $M = 0$, these are seen to be of the form

$$(\psi, b) = \mathrm{Re}\{\exp(i\lambda_i t)\exp(-i\alpha\xi)\,(\psi_n, b_n)\exp(in\phi)\}, \quad n = 0, \pm 1, \pm 2, \ldots .$$

Of great importance is the physical significance of (15). In §3.1, it was pointed out that, when $M = 0$, the disturbance equations describe freely propagating internal waves. From the relation of the ξ, η co-ordinate system to the non-dimensional x, y reference frame (see figures 1a, b), we see that the non-dimensional disturbance wavenumber referred to x, y co-ordinates is

$$(n\cos\theta - \alpha\sin\theta, n\sin\theta + \alpha\cos\theta).$$

If we define θ_n as the angle to the horizontal at which these free disturbance waves will propagate, we see from (6) that the (non-dimensional) frequency of that wave $\lambda_i - n\cos\theta$ is related to θ_n by

$$\cos\theta_n = \lambda_i - n\cos\theta.$$

Furthermore,

$$\cos\theta_n = (n\cos\theta - \alpha\sin\theta)/[(n\cos\theta - \alpha\sin\theta)^2 + (n\sin\theta + \alpha\cos\theta)^2]^{\frac{1}{2}}$$

from simple geometric considerations. Thus

$$\cos\theta_n = \lambda_i - n\cos\theta = (n\cos\theta - \alpha\sin\theta)/(n^2+\alpha^2)^{\frac{1}{2}}, \tag{16}$$

and we see that (15) can be retrieved by employing only physical arguments. For $M = 0$ and for a given mode (fixed value of n), (15) defines a curve along which there is an infinite set of (α, λ_i) pairs which are ostensibly candidates for the instability; however, only one pair will satisfy the additional restrictions imposed by increasing the order of the determinant in (14).

In §2, it was seen that, when $M = 0$, the points at which the stability curves cross the α axis were given by $\alpha = n^2$. This is a result with a great deal of intuitive appeal, for one would expect that the most unstable modes, those which can most readily extract energy from the basic state for their growth at finite M, would have wavenumbers which are related to harmonics of the solution of (1) when $M = 0$. In the present work, we expect that the lines of neutral stability will meet the α axis at points which are of similar importance when viewed in the context of energy transfer from the basic-state wave motion. For vanishingly small M, the waves which can grow at the expense of the basic-state energy are

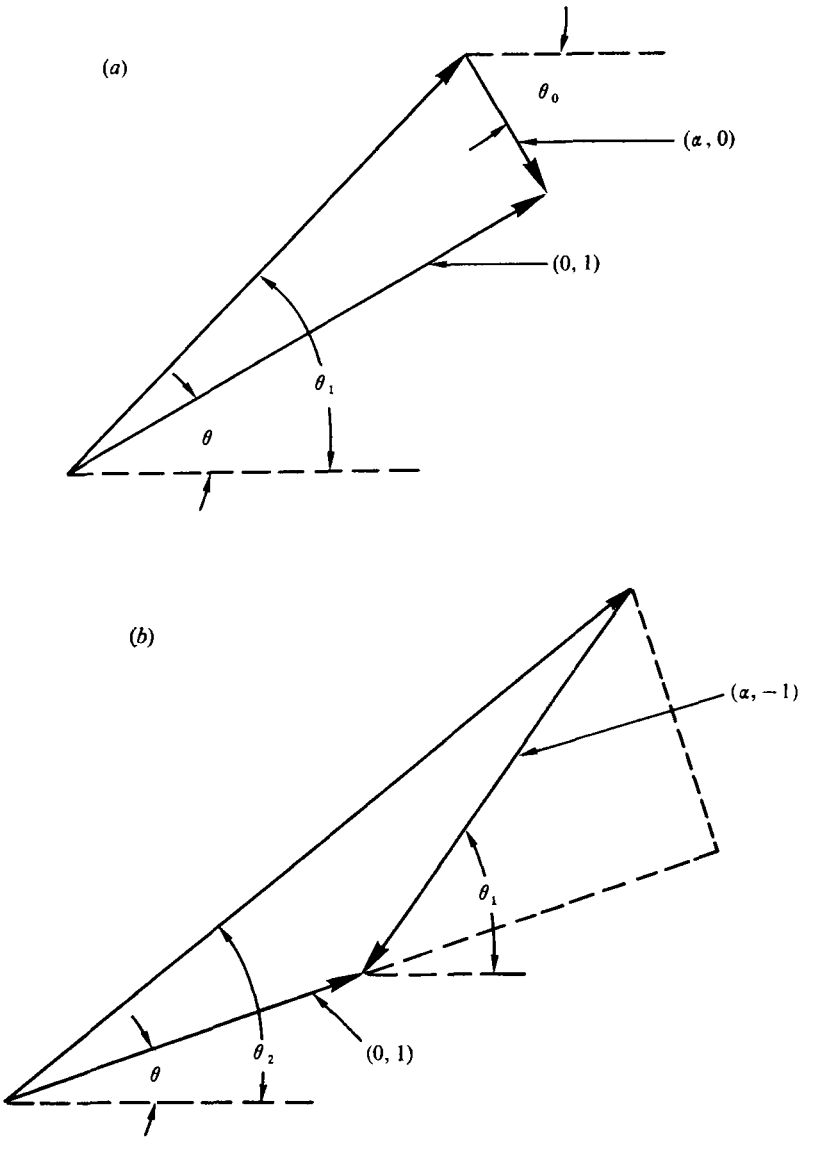

FIGURE 2. (*a*) The mechanism of the $n = 0, 1$ instability is that of the classical nonlinear resonant interaction when $M = 0$. (*b*) When $n = 1, 2$ the instability is that of a second-order resonant interaction with the respective participating waves more nearly collinear with the basic state.

those waves which participate in a nonlinear resonant interaction with the basic state given by (5).

The phase of the basic state is given by

$$\phi = \eta - t\cos\theta,$$

while the phases of the waves comprising the instability are seen from (11) to

Resonant waves ($M \simeq 0$)	α	λ_i
$n = 0, 1$	0·798	0·500
$n = 1, 2$	0·933	1·158
$n = 2, 3$	1·649	2·082

TABLE 2. The values of α and λ_i which satisfy the resonance condition (17) when $M = 0$. Here $\theta = 30°$ and $\beta = 90°$.

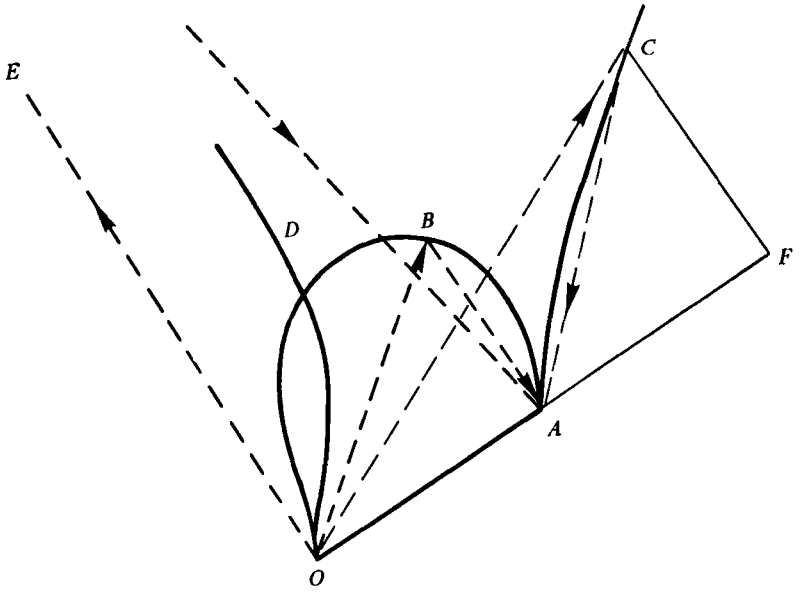

FIGURE 3. The heavy solid lines define the allowable nonlinear resonant sum interactions in which disturbances participate with the basic state OA. The resonance triad OBA constitutes the first parametric instability, the triangle OCA the second. The right-angled triangle OEA has point E lying on the curve ODE. This corresponds to a spurious root which is discussed in §3.2.

be $-\alpha\xi + n\eta + (\lambda_i - n\cos\theta)t$. The basic state and the disturbances† corresponding to $n = 0, +1$ are members of the resonant triad shown schematically in figure 2(*a*). These satisfy the resonance condition

$$\cos\theta_0 + \cos\theta_1 = \cos\theta$$

for only one value of α in general. We might suspect that this particular value of α corresponds to the first crossing point of a curve of neutral stability with the α axis; and indeed, this is shown in the next section to be the case. For $n = 1$ and 2 the unstable waves which participate in the three-wave resonant

† In what follows, the lower of the two integers will be used to refer to the disturbance. For example, an $n = 0, 1$ instability is said to correspond to $n = 0$.

interaction are pictured in figure 2(*b*) and again satisfy the resonance constraint

$$\cos\theta_1 + \cos\theta_2 = \cos\theta$$

for one α, which, as we shall see in the following section, is the second axis crossing point. Similar geometrical constructions which satisfy the frequency resonance condition may be formed in a similar fashion for all other integers $n \geqslant 2$. Each of these triads then permits resonance at second order for one value of α. Since there is a countably infinite set of such resonant triads, there is an infinitely denumerable set of α's for which the neutral-stability curves intersect the α axis (as is seen to be the case for Mathieu's equation). For a particular case ($\theta = 30°$) in the present problem, the first three intersection points are given in table 2.

In §3.1, β was fixed equal to 90°, and the ensuing analysis and above results follow from this assumption. The manner in which the countably infinite set of α's arise can be seen by examining figure 3, which displays the waves which satisfy the resonance conditions for participation in a second-order sum interaction with the basic state (Phillips 1966*a*). The resonance triad *OBA* corresponds to the first parametric instability, the triangle *OCA* to the second, and so forth. Clearly, the wave triad *OBA* can be distorted (by varying β) such that points *B* and *C* are co-incident. The infinitely denumerable set of α's which arise in the solution are thus artifacts of the restriction β = constant. Had we allowed β to vary, a continuum of unstable α's would have emerged as opposed to the discrete set obtained with the restriction β = constant.

Another right-angled triangle *OEA* can also be constructed such that point *E* lies on the curve *ODE*; this corresponds (when $\theta = 30°$) to a value of $\alpha \simeq 6{\cdot}67$. When $M > 0$ and $\lambda_r > 0$ however, no values along (or in the vicinity of) the curve *ODE* are found to be roots of the transcendental equation (14), so that the resonance conditions which define this particular curve are resonant interactions which are simply not contiguous to a region of parametric instability in the α, M parametric space.

When $M > 0$, these disturbances must propagate in the presence of a temporally and spatially modulated buoyancy field (the basic state). While one would not expect either (16) or the resonance condition

$$\cos\theta_n + \cos\theta_{n+1} = \cos\theta \tag{17}$$

to be valid for $M > 0$, there do exist instabilities which obey a resonance condition. These will be shown, however, to be members of a much larger set of instabilities, which are not in resonance with the basic state.

The *way* in which these particular (α, λ_i) pairs emerge from the calculations is indicated in figure 4 when the particular case $\theta = 30°$ is examined. The dispersion relation (15) is shown as a dashed line and the loci of zeros of $\mathrm{Re}\,\Delta$ and $\mathrm{Im}\,\Delta$ are also shown. The curves $\mathrm{Re}\,\Delta = 0$ are the lines running more or less parallel to the α axis, while the $\mathrm{Im}\,\Delta = 0$ lines are the loops entering from the left and right. The intersection points of these two families of curves represent roots of (14). We note that for each n there are two such roots, and that these are more or less equi-distant from the point of intersection of $\mathrm{Re}\,\Delta = 0$ and the dispersion curve (15). This is because the dispersion curve gives $\lambda_i = \lambda_i(\alpha)$ for

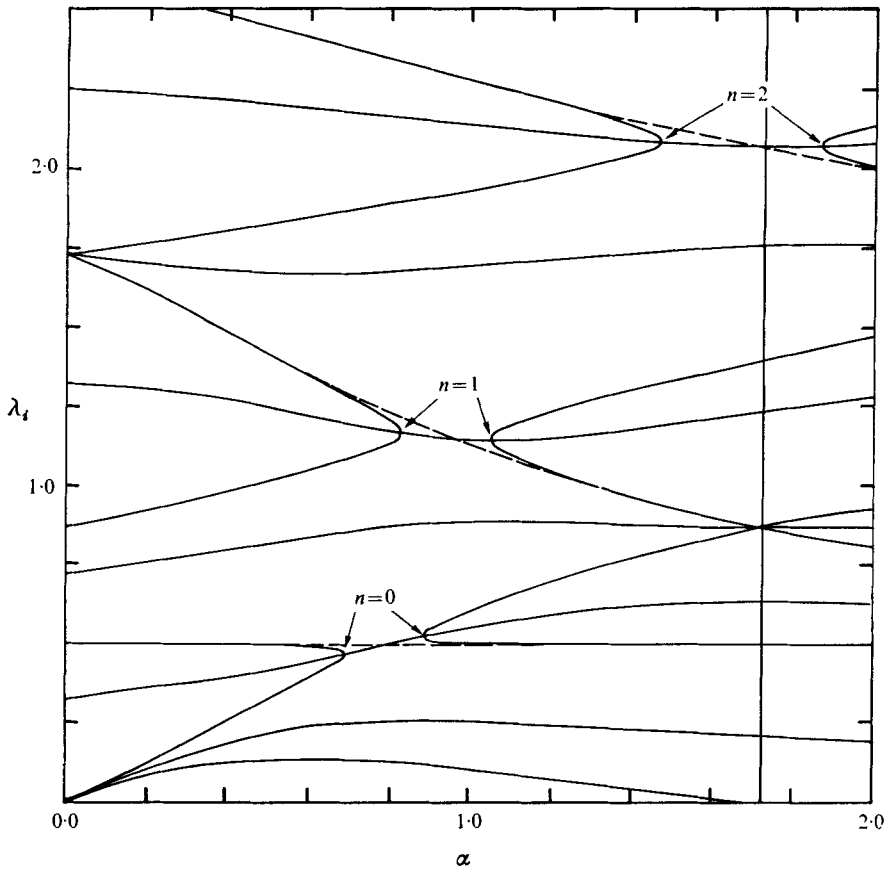

FIGURE 4. The α, λ_i plane for $M = 0{\cdot}1$ and $\lambda_r = 0{\cdot}01$. The intersection of the curves Re $\Delta = 0$ (the lines more or less parallel to the α axis) and Im $\Delta = 0$ (the loops entering from the left and right) define those points where $\Delta = 0$ for $\beta = 90°$, $\theta = 30°$ and $N = 11$. The locations of the roots for $n = 0, 1$ and 2 have arrows pointing towards them and their respective dispersion relations $\lambda_i = \lambda_i(\alpha)$ are given by dotted lines for $M = 0$ and $\lambda_r = 0$. See §3.2 for a more complete discussion.

$M = 0$, and this plot has been made for $M = 0{\cdot}1$. As M is increased above zero, the two roots (initially coincident when $M = 0$) become more distant in the α, λ_i plane, so that this behaviour gives rise to wedge-shaped regions of instability in the α, M plane. These V-shaped areas are analogous to those arising in Mathieu's equation.

The vertical line at $\alpha = +\sqrt{3}$ is a branch cut along which Re Δ and Im Δ are discontinuous, being infinite and of the opposite sign on either side of this line. This singularity arises naturally because of the occurrence of the factor

$$n\cos\theta - \alpha\sin\theta \tag{18}$$

in the denominator of various terms in (13). For $\theta = 30°$, (18) possesses roots at

$$\alpha = n\cot 30° = \sqrt{3}, 2\sqrt{3}, 3\sqrt{3}, \ldots,$$

which occur in the real and imaginary parts of the determinant.

Although roots of (14) have been found for the cases $n < 0$, examination of (15) shows them to be related to the $n \geqslant 0$ modes, at least when $M = 0$. That is, the transformation

$$(n, \alpha, \lambda_i) \rightarrow (-n, -\alpha, -\lambda_i)$$

leaves (15) unaltered. Numerically, it is observed for $M > 0$ that

$$\psi_n(\alpha, \lambda_i) = \psi^*_{-n}(-\alpha, -\lambda_i),$$

where the asterisk denotes a complex conjugate. Thus the $n \geqslant 0$ modes appear in the region $\alpha > 0$, $\lambda_i > 0$ (shown in figure 4), while the quadrant $\alpha < 0$, $\lambda_i < 0$ contains essentially the same roots which correspond to $n \leqslant 0$.

3.3. *The numerical approach*

When $M \neq 0$, the problem is essentially one of choosing the parameters α, M, λ_r, λ_i and θ in such a fashion that the relations

$$\mathrm{Re}\,\Delta = 0, \quad \mathrm{Im}\,\Delta = 0 \tag{19a, b}$$

are valid. This requires a careful search of the parameter space and we proceed by rewording, in effect, the question posed at the conclusion of §3.1. First we fix θ, λ_r and α. In the λ_i, M plane, we then examine the locus of points such that (19*a*) or (19*b*) is satisfied. At the crossing of these two curves the complex magnitude of the determinant vanishes, hence (14) is satisfied. Cycling through values of α and repeating this search for the roots of (14) in the λ_i, M plane, we obtain a sequence of triads (α, M, λ_i) for which the determinant vanishes. Since we have fixed λ_r and θ for this calculation, we have obtained the curves of constant growth rate $M = M(\alpha; \lambda_r)$ for a wave propagating at angle θ to the horizontal; we also know the dispersion relation $\lambda_i = \lambda_i(\alpha)$ of the instability.

The evaluation of the complex determinant is performed numerically using the method of Gaussian elimination (Noble 1969) to form a triangular matrix, so that the determinant is then the product of the diagonal terms. By successively halving the size of a box in the λ_i, M plane, the roots of the determinant may be located to within an arbitrary accuracy in this plane. We have seen in §2 that as the order of the determinant N is increased the accuracy of the neutral-stability curves is increased, their position in the λ_i, M plane converging as N becomes large. By increasing N and noting any change in the position of the $M = M(\alpha; \lambda_r)$ curves, we are able to establish a minimum determinant size to be used in the calculations for any given error criterion. For $M \lesssim O(\frac{1}{3})$, the position of the curves was found to be accurate to within a nominal 1% provided $N \geqslant 11$.

Using the parameter-search technique described above, we find that internal waves exhibit qualitatively similar parametric instabilities for all values of θ sampled between 10° and 80°. As the properties of these disturbances are similar for all θ, only one representative example ($\theta = 30°$) is examined extensively.

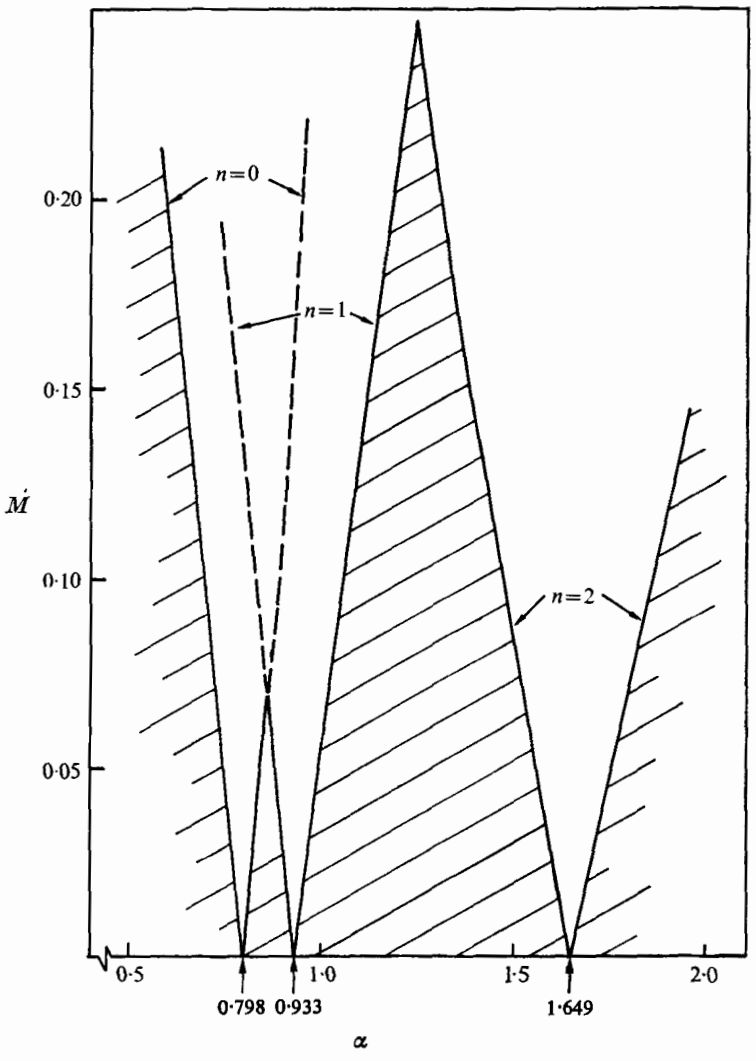

FIGURE 5. The curves of neutral stability separate the α, M plane into regions of instability and stability, the latter appearing as the shaded areas. These neutral curves correspond to the modes $n = 0$, 1 and 2 when $\beta = 90°$, $\theta = 30°$ and $N = 11$.

4. Discussion of results for the case $\theta = 30°$

The curves of neutral stability ($\lambda_r = 0$) are shown in figure 5 for the first three modes, $n = 0$, 1 and 2; note that the values of α at which these curves intersect the axis are precisely those given in table 2. These neutral curves form an irregular sawtooth pattern and divide the plane into regions of stability and instability. In this respect, these wedge-like regions qualitatively resemble those arising from a similar treatment of Mathieu's equation. They differ, however, in that the various branches cross one another. This should not be considered particularly surprising, as these various branches correspond to different

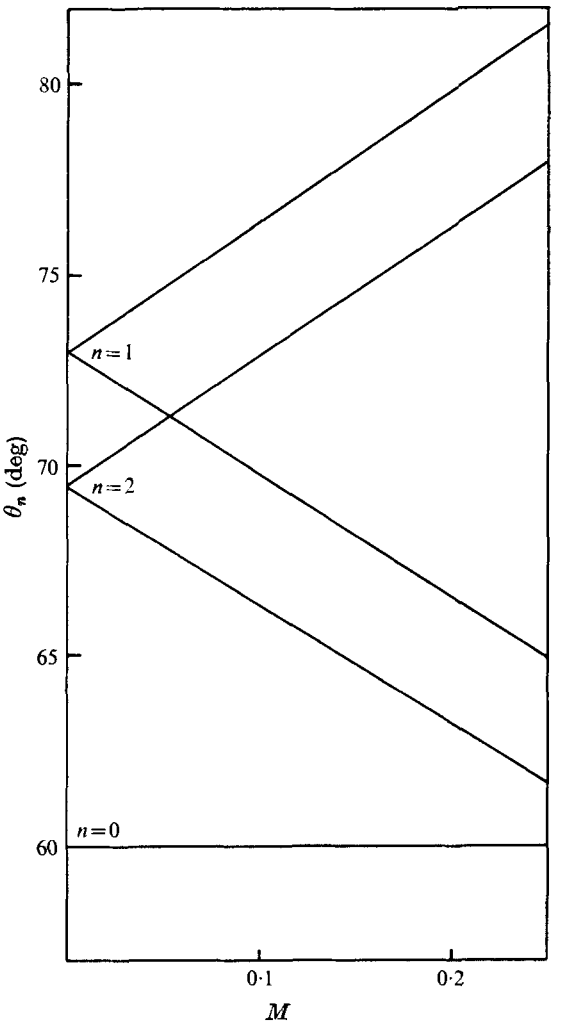

FIGURE 6. The disturbance phase propagation direction θ_n is shown as a function of the basic-state M for $n = 0, 1$ and 2. Here $\beta = 90°$, $\theta = 30°$ and $N = 11$. The θ_n are measured as indicated in figures 2(*a*) and (*b*).

frequencies and therefore represent waves propagating at different angles from one another (see figures 2*a*, *b*).

For $M = 0$, the dispersion relation of the disturbance is shown in §3.2 to be

$$\cos\theta_n = \lambda_i - n\cos\theta = (n\cos\theta - \alpha\sin\theta)/(n^2+\alpha^2)^{\frac{1}{2}}.$$

The frequency and angle of propagation of these waves are simply related by linear theory. That is, this dispersion relation is equivalent to (6) for waves propagating in an otherwise quiescent fluid. For $M > 0$, however, these disturbance waves must propagate through a medium which is already supporting the buoyancy and velocity fluctuations associated with the passage of the large-amplitude basic-state wave. While it is geometrically obvious that

$$\cos\theta_n = (n\cos\theta - \alpha\sin\theta)/(n^2+\alpha^2)^{\frac{1}{2}}, \tag{20}$$

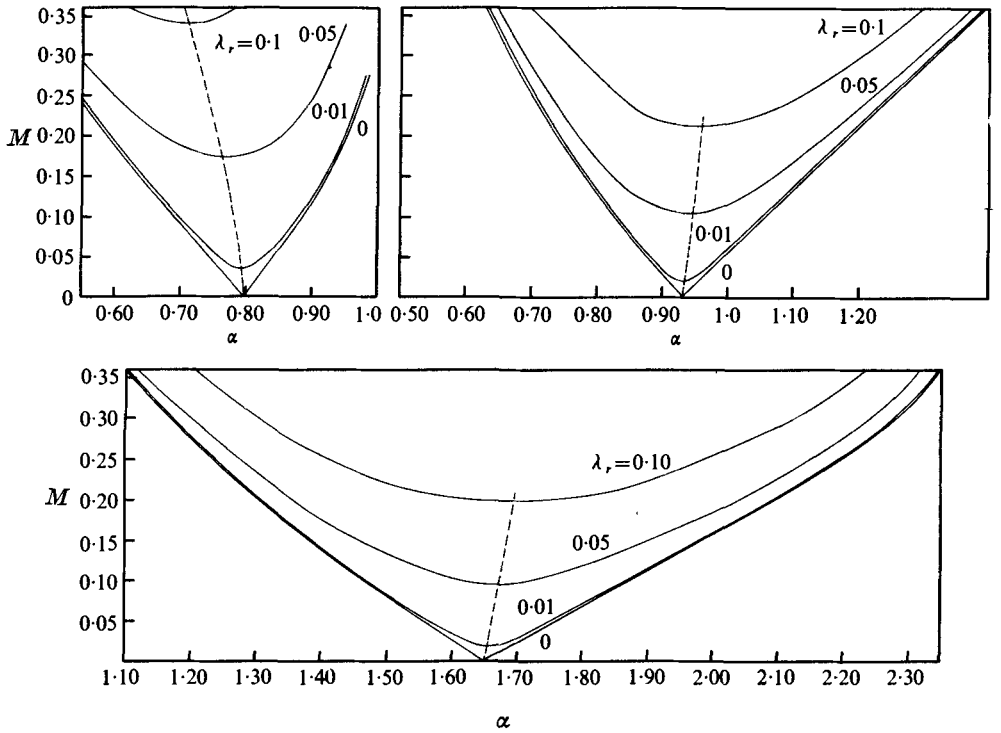

FIGURE 7. The curves of constant growth rate λ_r for (clockwise from upper left) $n = 0$, 1 and 2. Here $\beta = 90°$, $\theta = 30°$ and $N = 11$. The dashed lines give the location of the maximum λ_r for the disturbance at that value of M.

we would not expect, nor indeed do we find, that the propagation direction and frequency are related in the classical fashion given by (6). In general then,

$$\cos\theta_n \neq \lambda_i - n\cos\theta, \quad M > 0.$$

Because of the parameter search employed to solve (14), α and M are known for $\theta = 30°$ and $\lambda_r = 0$. Using (20), we can calculate $\theta_n = \theta_n(M)$ for the down-going waves (see figures 2*a*, *b*) associated with the first three unstable modes, and the results of this calculation are displayed in figure 6.

The significant result obtained here is that this instability is a fundamentally nonlinear one which involves mode coupling and the concomitant transfer of energy from the basic state into the disturbance. As a measure of the rate of growth of those disturbances, we have calculated the curves λ_r = constant. In figure 7, we display these curves of constant growth rate $M = M(\alpha; \lambda_r)$ for $\lambda_r = 0{\cdot}0$, $0{\cdot}01$, $0{\cdot}05$ and $0{\cdot}10$, and $n = 0$, 1 and 2. We note that a qualitative difference appears between growth-rate families for the different modes n. The minimum M on a curve λ_r = constant appears to shift to larger or smaller α as λ_r is increased, depending on which mode we are discussing. The loci of points for which the minimum M occurs on curves of constant growth rate are shown in figure 7 as dashed lines, which pass through the vertex of the V-shapes formed by the neutral curves at the $M = 0$ axis.

In this work, we have simply put $\beta = 90°$ so that the Floquet vector with magnitude $|\alpha\mathbf{k}|$ is perpendicular to the basic-state vector $\mathbf{k}$ (see figure 1*b*). This choice of β was made simply for the sake of definiteness, and because it is financially prohibitive to perform anything other than a few sample calculations with a variety of values of β. Another choice of β would have yielded another, similar, set of instabilities, each with their own growth rates, and these will turn out to grow faster or slower than the instabilities whose growth rates are exhibited in figure 7. So we see that, at the very worst, the choice $\beta = 90°$ may lead one to underestimate the maximum disturbance growth rates available in the system (9*a*, *b*). On the other hand, we can say with absolute certainty that, of all the available instabilities, there exist disturbances which will grow *at least as rapidly* as the ones shown in figure 7. Moreover, the essential features of the instability remain qualitatively the same for $\beta \neq 90°$: plane internal waves of even vanishingly small amplitude are parametrically unstable.

The countably infinite disturbance wavenumber set (with $\beta = 90°$), expressed in the ξ, η frame, is

$$\mathbf{k}_n = (\alpha, n), \quad n = 0, 1, 2, \ldots,$$

so that $|\mathbf{k}_n| = (\alpha^2 + n^2)^{\frac{1}{2}}$. Recall that these have been non-dimensionalized with the basic-state wavenumber $|\mathbf{k}|$, so that $|\mathbf{k}_n|$ represents the ratio of the basic-state wavelength to that of the disturbance. For the case $n = 0$ only, we see that the wavelength of the smaller wavenumber instability ($= 2\pi/\alpha$) *exceeds* that of the basic state. In fact, preliminary calculations reveal that the $n = 0$ mode exhibits this trend for all values of θ between 10° and 80°, so that this behaviour is not confined only to the case $\theta = 30°$. Among all the different modes, the $n = 0$ case is unique in this respect. We remark further that the long wavelength feature of the $n = 0$ mode is in contrast to the type of instability uncovered by McEwan & Robinson (1975), who considered only instabilities having much smaller length scales than the basic-state wave. The present work does, however, seem to support McEwan & Robinson's choice of the small-scale waves as those most likely to render the basic state unstable. Evidence of this is seen in figure 7, where we note that the minimum value of M (on any curve of constant growth rate) becomes smaller as n is increased. It is important to comment in this regard on the importance of viscosity. If M is kept constant and successively higher modes are examined, one may obtain values of the maximum λ_r (which lie along the dashed lines in figure 7) and its associated α, from which $|\mathbf{k}_n|$ may be calculated. In so doing, we observe that $\max\{\lambda_n(|\mathbf{k}_n|), M = \text{constant}\}$ does not rise as rapidly as the rate of viscous dissipation, which is proportional to $|\mathbf{k}_n|^2$. For basic states of very small wavelength then, the lower-order modes would be the most unstable, as their viscosity-adjusted growth rate is larger than that for the higher modes. For oceanic waves having wavelengths of the order of tens of metres on the other hand, it would appear that the higher modes are indeed the most unstable, as viscosity would only seriously influence the behaviour of *very* high mode number instabilities, having commensurately small wavelengths.

While any discussion involving extrapolated growth rates must be viewed as conjectural, it is important to state that for the larger n, the resonant triads for

$M \simeq 0$ (see figures 2*a*, *b* and 3) become more nearly collinear. Phillips (1966*b*) has shown that, for nearly collinear waves, the interaction times are shorter than those for waves arranged in a more nearly equilateral configuration. Since, for finite M, the instability is in general merely a detuned resonant interaction with a finite-amplitude basic state, there is some basis for the conjecture that the trend of increasing disturbance growth rate with higher mode number would continue past the cases represented in this paper.

These calculations have been performed for $M \leqslant O(\frac{1}{3})$ not only to keep the determinant size no greater than $N = 11$ for accuracy, but because different *types* of internal-wave instabilities seem to occur for values of M significantly larger than this. These disturbances possess stability curves qualitatively different from those of parametric instabilities; furthermore, their existence at these higher values is not explained by the theory of §3. A concern more germane to the present work, however, is the possibility that internal waves may exhibit subharmonic parametric instabilities. In fact, there is no reason to believe that subharmonic instabilities do not exist; although, in a sense, the question may be moot because numerical calculations have been made which exhibit instabilities for all waves with $10° \leqslant \theta \leqslant 80°$ whenever $0 < M \ll 1$. More significantly, however, we cannot dismiss the possibility that subharmonic modes might possess growth rates which exceed those of the harmonic ones considered in this paper. Since the lower mode numbers of the harmonic instabilities seem to require larger values of M to produce the same disturbance growth rate, we might conjecture that these longer subharmonic instabilities, if indeed they exist, are probably not as important as the harmonic ones. Only the actual analysis of the problem, however, can resolve the question.

5. Conclusion

We have solved the problem of the harmonic parametric instability of a finite-amplitude plane internal gravity wave in an incompressible Boussinesq fluid, and this parametric instability has been shown to reduce to the classical second-order nonlinear resonant interaction in the limit of vanishingly small basic-state amplitude. Although only the case for waves propagating at an angle $\theta = 30°$ to the horizontal has been examined in detail, preliminary calculations have been made for a variety of values of θ between 10° and 80° with the same qualitative results. As was discussed in the previous section, the restriction $\beta = 90°$ may cause us to underestimate the disturbance growth rates somewhat, but this does not vitiate the principal conclusion of this work as regards the stability of internal waves. We conclude, therefore, that even infinitesimal-amplitude internal waves for which $10° < \theta < 80°$ are parametrically unstable. Of these unstable modes, the limited evidence presented in this paper suggests that those with the higher wavenumbers are the faster-growing disturbances.

The reader should bear in mind, however, the *caveat* of §3.2 regarding β. For a finite-amplitude internal wave, instabilities develop and grow simultaneously over a wide range of angles β. These instabilities, acting in concert, extract the energy of the basic state at such a rate that they appreciably alter its amplitude and thus rapidly invalidate the linearization.

The author expresses his gratitude to Dr T. H. Bell Jr, and Dr J. P. Dugan of the Naval Research Laboratory for a number of provocative discussions on this problem.

Appendix

The recursion relation

$$-M\psi_{n-2}+(\alpha-n^2)\psi_n-M\psi_{n+2}=0$$

links three non-contiguous coefficients. Substitution of the integer values $n=0,\pm1,\pm2,\ldots$ yields a linear homogeneous algebraic system of infinite order. The necessary condition for the existence of a non-trivial solution is that the associated infinite determinant vanishes:

$$\Delta(\alpha,M;N=\infty)=\begin{vmatrix} . & . & . & . & . & . & . & . & . \\ \ldots & \alpha-9 & 0 & -M & 0 & 0 & 0 & 0 & \ldots \\ \ldots & 0 & \alpha-4 & 0 & -M & 0 & 0 & 0 & \ldots \\ \ldots & -M & 0 & \alpha-1 & 0 & -M & 0 & 0 & \ldots \\ \ldots & 0 & -M & 0 & \alpha & 0 & -M & 0 & \ldots \\ \ldots & 0 & 0 & -M & 0 & \alpha-1 & 0 & -M & \ldots \\ \ldots & 0 & 0 & 0 & -M & 0 & \alpha-4 & 0 & \ldots \\ \ldots & 0 & 0 & 0 & 0 & -M & 0 & \alpha-9 & \ldots \\ . & . & . & . & . & . & . & . & . \end{vmatrix}=0.$$

The case $N=3$ leads to

$$\Delta(\alpha,M;N=3)=\alpha[(\alpha-1)^2-M^2]=0,$$

and so the first approximations to the neutral branches are

$$\alpha=O(M^2),\quad \alpha=1-M+O(M^2),\quad \alpha=1+M+O(M^2).$$

Along these branches, the solutions

$$\begin{aligned}\psi&=\mathrm{ce}_0(\eta,M)=2^{-\frac{1}{2}}[1-\tfrac{1}{2}M\cos 2\eta+O(M^2)],\\ \psi&=\mathrm{se}_1(\eta,M)=\sin\eta+O(M),\\ \psi&=\mathrm{ce}_1(\eta,M)=\cos\eta+O(M),\end{aligned}$$

respectively, are valid (Abramowitz & Stegun 1965). Proceeding with the next higher approximation, we find that

$$\Delta(\alpha,M;N=5)=(\alpha-4)[(\alpha-1)^2-M^2][\alpha(\alpha-4)-2M^2]=0,$$

which has solutions

$$\begin{aligned}&\alpha=1-M+O(M^2),\quad \alpha=1+M+O(M^2),\\ &\alpha=-\tfrac{1}{2}M^2+O(M^4),\quad \alpha=4+\tfrac{1}{2}M^2+O(M^4),\\ &\alpha=4+O(M).\end{aligned}$$

No new information is gained regarding the parametric relations for ce_1 and se_1, but the third $\alpha(M)$ represents a refinement in the accuracy of the ce_0 curve, while

the latter two are new curves. These correspond to

$$\psi = \mathrm{ce}_2(\eta, M) = \cos 2\eta + O(M),$$
$$\psi = \mathrm{se}_2(\eta, M) = \sin 2\eta + O(M),$$

respectively, but we remark that $\alpha = 4 + \frac{1}{2}M^2 + O(M^3)$ is in error by $\frac{1}{12}M^2$, the precise answer being $\alpha = 4 + \frac{5}{12}M^2 + O(M^3)$. The case $N = 7$ yields

$$\Delta(\alpha, M; N = 7) = (\alpha - 4)[\alpha(\alpha - 4) - 2M^2]\{[(\alpha - 1)(\alpha - 9) - M^2]^2 - M^2(\alpha - 9)^2\}$$
$$= 0.$$

The second factor, which yields the curve for ce_2, still yields a neutral curve which is in error by $\frac{1}{12}M^2$, but the last factor improves the accuracy of our knowledge of the se_1 and ce_1 curves:

$$\alpha = 1 - M - \tfrac{1}{8}M^2 + O(M^3)$$

and

$$\alpha = 1 + M - \tfrac{1}{8}M^2 + O(M^3).$$

In addition, the last factor introduces the stability boundaries for ce_3 and se_3. To $O(M^3)$, they are identical:

$$\alpha = 9 + \tfrac{1}{8}M^2 + O(M^3).$$

REFERENCES

Abramowitz, M. & Stegun, I. A. 1965 *Handbook of Mathematical Functions*. Dover.

Booker, J. R. & Bretherton, F. P. 1967 The critical layer for internal gravity waves in a shear flow. *J. Fluid Mech.* **27**, 513–539.

Breeding, R. J. 1971 A nonlinear investigation of critical levels for internal atmospheric gravity waves. *J. Fluid Mech.* **50**, 545–563.

Charnock, H. 1965 A preliminary study of the directional spectrum of short period internal waves. In *Proc. 2nd U.S. Navy Symp. Military Oceanography*, pp. 175–178.

Davis, H. T. 1962 *Introduction to Nonlinear Differential and Integral Equations*. Dover.

Garrett, C. & Munk, W. 1972 Space-time scale of internal waves. *Geophys. Fluid Dyn.* **3**, 225–264.

Gill, A. E. 1974 The stability of planetary waves on an infinite beta-plane. *Geophys. Fluid Dyn.* **6**, 29–47.

Ince, E. L. 1956 *Ordinary Differential Equations*. Dover.

McEwan, A. D. & Robinson, R. M. 1975 Parametric instability of internal gravity waves. *J. Fluid Mech.* **67**, 667–687.

Mied, R. P. & Dugan, J. P. 1974 Internal gravity wave reflection by a layered density anomaly. *J. Phys. Ocean.* **4**, 493–498.

Mied, R. P. & Dugan, J. P. 1975 Internal wave reflection by a velocity shear and density anomaly. *J. Phys. Ocean.* **5**, 279–287.

Noble, B. 1969 *Applied Linear Algebra*. Prentice-Hall.

Orlanski, I. 1971 Energy spectrum of small-scale internal gravity waves. *J. Geophys. Res.* **76**, 5829–5835.

Orlanski, I. 1972 On the breaking of standing internal gravity waves. *J. Fluid Mech.* **54**, 577–598.

Orlanski, I. & Bryan, K. 1969 Formation of the thermocline step structure by large amplitude internal gravity waves. *J. Geophys. Res.* **74**, 6975–6983.

Phillips, O. M. 1966*a* *The Dynamics of the Upper Ocean*. Cambridge University Press.

PHILLIPS, O. M. 1966*b* Internal wave interactions. In *Proc. Sixth Symp. Nav. Hyd.* (ed, R. D. Cooper & S. W. Doroff), pp. 535–544. Office of Naval Research, Dept. Navy, publ. ARC-136.

PHILLIPS, O. M. 1968 The interaction trapping of internal gravity waves. *J. Fluid Mech.* **34**, 407–416.

THORPE, S. A. 1975 The excitation, dissipation, and interaction of internal waves in the deep ocean. *J. Geophys. Res.* **80**, 328–338.